

Efficient Low-Memory Fast Stack Decoding with Variance Polarization for PAC Codes

Mohsen Moradi¹, Hessam Mahdavi¹

Abstract—Polarization-adjusted convolutional (PAC) codes have recently emerged as a promising class of error-correcting codes, achieving near-capacity performance particularly in the short block-length regime. In this paper, we propose an enhanced stack decoding algorithm for PAC codes that significantly improves parallelization by exploiting specialized bit nodes, such as rate-0 and rate-1 nodes. For a rate-1 node with N_0 leaf nodes in its corresponding subtree, conventional stack decoding must either explore all 2^{N_0} paths, or, same as in fast list decoding, restrict attention to a constant number of candidate paths. In contrast, our approach introduces a pruning technique that discards wrong paths with a probability exponentially approaching zero, retaining only those whose path metrics remain close to their expected mean values. Furthermore, we propose a novel approximation method for estimating variance polarization under the binary-input additive white Gaussian noise (BI-AWGN) channel. Leveraging these approximations, we develop an efficient stack-pruning strategy that selectively preserves decoding paths whose bit-metric values align with their expected means. This targeted pruning substantially reduces the number of active paths in the stack, thereby decreasing both decoding latency and computational complexity. Numerical results demonstrate that for a PAC(128, 64) code, our method achieves up to a 70% reduction in the average number of paths without degrading error-correction performance.

Index Terms—PAC codes, polar codes, stack decoding, varentropy, polarization, mutual information, sequential decoding.

I. INTRODUCTION

POLAR codes are the first class of error-correcting codes that theoretically achieve the capacity of memoryless symmetric channels [1]. However, at short block lengths, their error-correction performance (ECP) falls short of the theoretical limits. The recently introduced polarization-adjusted convolutional (PAC) codes [2], which enhance polar codes via pre-coding with convolutional codes, exhibit an ECP that closely approaches the theoretical bounds at short block length regimes when decoded using sequential decoding algorithms [2], [3]. PAC codes can also be viewed as a combination of polar codes and cyclic codes [4]. PAC codes can be decoded using various tree-search algorithms, such as sequential decoding.

As a sequential decoding algorithm, the stack algorithm [5], [6] evaluates the most likely path in the stack, computes the metric values for both of its branches, and adds them to the stack after removing that path. Since the stack algorithm can revisit certain levels of the decoding tree multiple times,

adding both branches at each step can greatly increase the number of paths in the stack, complicating the identification of the most likely path and increasing the decoding delay. In this paper, we introduce a stack-pruning method that identifies bifurcated branches unlikely to belong to the correct path, thus preventing their addition to the stack. Our results demonstrate that a pruning approach significantly reduces the average number of paths in the stack, thereby improving both decoding complexity and delay.

Our stack-pruning technique benefits from the concept of metric function polarization introduced in [7], where it is shown that at each step of the polarization process, the mean and variance of the metric function random variable correspond to the polarized mutual information and varentropy of the synthesized binary input discrete memoryless channel (BI-DMC), respectively. For a binary input additive white Gaussian noise (BI-AWGN) channel, [8] proposes an algorithm to calculate the polarized mutual information, which can also be used to compute the polarized channel varentropy [7]. In [7], also an approximation method for calculating the varentropy of the BI-AWGN channel is introduced. Following the approach in [9], in this paper, we also assume that the channel remains a BI-AWGN channel after each polarization step. Using the method outlined in [7], we propose a technique to compute the polarized varentropies of the synthesized BI-AWGN channels at each step of the polarization. Numerical results show that the polarized varentropy values obtained from our approximation method closely match those derived using the method from [8].

Using our proposed approximation for the polarized mutual information and polarized varentropy of the BI-AWGN channel, we introduce a stack decoding method that prunes branches falling below a certain threshold. Our stack-pruning method integrates the approaches proposed in [10] and [7]. In [10], it was shown using the Chernoff bound that the probability of pruning the correct path, i.e., the probability that the correct path's metric falls below the threshold, decreases exponentially with the threshold in the exponent. Similarly, in [7], using the Chebyshev bound, it was demonstrated that the probability of the correct path's metric deviating from the polarized mutual information by more than the threshold is upper bounded by a ratio, with the polarized channel varentropy in the numerator and the square of the threshold in the denominator.

After polarization, we observe that for certain polarized channels, the Chebyshev bound provides a tighter threshold, while for others, the Chernoff bound yields a better result. Leveraging both bounds, along with our proposed polarized varentropy approximation, we introduce a pruning method that

The authors are with the Department of Electrical & Computer Engineering, Northeastern University, Boston MA-02115, USA (e-mail: m.moradi@northeastern.edu, h.mahdavi@northeastern.edu).

This work was supported by NSF under Grant CCF-2415440 and the Center for Ubiquitous Connectivity (CUBIC) under the JUMP 2.0 program.

excludes paths with metric values below the underlying threshold, which is determined based on a suitable method out of the two methods mentioned above. Numerical results demonstrate that for a PAC(128, 64) code, our proposed pruning method achieves a 70% reduction in the average number of paths in the stack compared to the conventional stack algorithm, and an 18% improvement compared to the method in [10] at 1 dB E_b/N_0 .

To enhance the parallelism of our proposed stack-pruning algorithm, we leverage four types of special nodes: rate-0, rate-1, rate-IV and repetition (REP) nodes. A rate-1 node with N_0 leaf nodes can generate 2^{N_0} candidate paths in the conventional stack decoding algorithm. In [11], a fast block stack decoding method for polar codes is introduced, which recommends retaining only 4 out of the 2^{N_0} possible paths to avoid significant ECP loss. In polar codes, the rate profile is typically constructed based on the reliability of the polarized bit-channels, and retaining 4 paths generally preserves ECP performance. However, for short block-length PAC codes, a rate profile based on alternative criteria—such as the weight distribution of the code—is often more favorable [3]. In our approach, for rate-1 nodes, we apply a stack-pruning strategy that permits bifurcation only when the corresponding child node has a bit metric exceeding our proposed threshold. For REP nodes, which yield two candidate paths, we retain a path only if the bit metric of its final leaf node exceeds its associated threshold. Our proposed algorithm for handling rate-IV and repetition (REP) special nodes can also be seamlessly applied to any other rate profile regardless of the particular strategy to select information-bit positions. Such nodes are investigated in the context of SCL decoding in [12]. In particular, since the pruning and metric-update rules we introduce do not depend on a particular rate profile structure, the method remains applicable even when the bit-channel ordering or information set is tailored to alternative design criteria. Our contributions in this paper can be summarized as follows:

- **Approximation of Polarized Varentropy:** We develop an efficient approximation for estimating the polarized channel varentropy of a BI-AWGN channel in $O(\log_2(N))$ time. This approximation enables fast and accurate computation of adaptive pruning thresholds without compromising decoding performance.
- **Hybrid Path-Pruning Strategy:** We propose a novel pruning method that exploits the polarization properties of the bit-metric function to discard low-probability decoding paths while guaranteeing that the probability of discarding the correct path decreases exponentially. By combining insights from both Chebyshev and Chernoff bounds, our method dynamically selects the tighter threshold for each bit-channel, resulting in a more effective and adaptive pruning method.
- **Fast Stack Decoding Algorithm for PAC Codes:** We design an efficient fast stack decoding algorithm for PAC codes that seamlessly integrates the proposed pruning strategy and supports the handling of rate-0, REP, type-IV, and rate-1 special nodes. For rate-1 nodes, where conventional stack decoding may require exploring up to

2^{N_0} candidate paths—which can be prohibitively large for high-rate PAC codes—our pruning-based approach significantly reduces computational complexity while maintaining near-optimal error-correction performance.

The remainder of this paper is organized as follows. Section II reviews the necessary background and preliminaries to make the paper self-contained. In Section III, we discuss the polarization of channel parameters and introduce an approximation method for estimating the polarized varentropy. Section IV presents our proposed pruning strategy, which selectively removes unlikely decoding paths from the stack based on adaptive thresholds. In Section V, we introduce the fast stack decoding algorithm, which efficiently handles different types of special nodes and integrates the proposed pruning method to reduce decoding complexity. Finally, Section VI provides numerical results demonstrating the performance gains and computational benefits of the proposed techniques.

II. PRELIMINARIES

A. Notation Convention

Vectors and matrices are represented in this paper by bold-face letters. All operations are performed in the binary field \mathbb{F}_2 . For a vector $\mathbf{u} = (u_1, u_2, \dots, u_N)$, subvectors (u_1, \dots, u_i) and (u_i, \dots, u_j) are denoted by \mathbf{u}^i and \mathbf{u}_i^j , respectively. For a given set \mathcal{A} , the subvector $\mathbf{u}_{\mathcal{A}}$ includes all elements u_i where i belongs to the set \mathcal{A} .

B. PAC Coding Scheme

A PAC code can be characterized by the parameters $(N, K, \mathcal{A}, \mathbf{c}(t))$, where $N = 2^n$ is the code length, K is the data length, \mathcal{A} defines the location of the data bits (known as the rate profile), and $\mathbf{c}(t)$ is the connection polynomial that specifies the convolutional code within the PAC code. During encoding, the data vector \mathbf{d} is first embedded into the data carrier vector \mathbf{v} such that $\mathbf{v}_{\mathcal{A}} = \mathbf{d}$ and $\mathbf{v}_{\mathcal{A}^c} = \mathbf{0}$. A one-to-one convolutional encoder, derived from the connection polynomial, then maps the data carrier vector \mathbf{v} to the vector \mathbf{u} . Subsequently, the polar transform maps \mathbf{u} to the encoder output \mathbf{x} as $\mathbf{x} = \mathbf{u}\mathbf{F}^{\otimes n}$, where $\mathbf{F} = \begin{bmatrix} 1 & 0 \\ 0 & 1 \end{bmatrix}$ and \otimes denotes the Kronecker power. With binary phase shift keying (BPSK) modulation over a BI-AWGN channel, the channel output is represented by the vector \mathbf{y} . A stack decoder is employed to estimate the vector $\hat{\mathbf{v}}$, from which the estimate of the data vector is retrieved using the rate profile. The frame error rate (FER), defined as $P(\hat{\mathbf{d}} \neq \mathbf{d})$, serves as the key metric to evaluate the system performance.

C. Channel Parameters

For a BI-DMC $W : \mathcal{X} \rightarrow \mathcal{Y}$, where \mathcal{Y} represents the output alphabet, the channel transition probability is denoted by $W(y|x)$, with $y \in \mathcal{Y}$ and $x \in \mathcal{X} = \{0, 1\}$. The channel cutoff rate for a uniform input distribution is defined as

$$R_0(W) \triangleq 1 - \log_2 \left(1 + \sum_{y \in \mathcal{Y}} \sqrt{W(y|0)W(y|1)} \right). \quad (1)$$

Another important parameter of the channel W is the symmetric channel capacity, defined as

$$I(W) \triangleq \sum_{x \in \mathcal{X}} \sum_{y \in \mathcal{Y}} p(x, y) \log_2 \left(\frac{p(y|x)}{p(y)} \right). \quad (2)$$

The varentropy of the channel W is also defined as

$$\text{Var}(W) \triangleq \sum_{x \in \mathcal{X}} \sum_{y \in \mathcal{Y}} p(x, y) \log_2^2 \left(\frac{p(y|x)}{p(y)} \right) - I(W)^2. \quad (3)$$

D. Stack Decoding

In a sequential decoding algorithm, the decoder bifurcates only the best path, i.e., the path with the best path metric value. As a sequential decoding algorithm, the stack algorithm maintains all previously evaluated paths in a stack. For PAC codes, the stack decoding procedure is described in Algorithm 1.

Algorithm 1 Stack Algorithm for PAC Code

- 1: **Initialize** the stack with the single-node path starting from the origin with path metric of 0.
 - 2: **while** the top path has not reached a leaf node **do**
 - 3: **Pop** the top path from the stack.
 - 4: **if** the current node corresponds to an information bit **then**
 - 5: **Compute** the path metric values for both immediate successors.
 - 6: **else**
 - 7: **Compute** the path metric value for the single immediate successor.
 - 8: **end if**
 - 9: **Push** the successor(s) to the stack with their associated metric values.
 - 10: **Reorder** the stack in descending order of the path metric values.
 - 11: **end while**
 - 12: **Output** the top path as the decoded path.
-

E. Path Metric

For a code of length N , after polarization, one can obtain N synthesized channels $W_N^{(i)} : \mathcal{X} \rightarrow \mathcal{Y}^N \times \mathcal{X}^{i-1}$ from N copies of the channel W [1]. The path metric for the stack decoding at level j is defined in [13] as

$$\Gamma(\mathbf{u}^j; \mathbf{y}) = \sum_{i=1}^j \gamma(u_i; \mathbf{y}, \mathbf{u}^{i-1}), \quad (4)$$

where

$$\begin{aligned} \gamma(u_i; \mathbf{y}, \mathbf{u}^{i-1}) &= \log_2 \frac{P(\mathbf{y}, \mathbf{u}^{i-1} | u_i)}{P(\mathbf{y}, \mathbf{u}^{i-1})} - R_0(W_N^{(i)}) \\ &= 1 - \log_2 \left(1 + 2^{-L_i \cdot (-1)^{u_i}} \right) - R_0(W_N^{(i)}), \end{aligned} \quad (5)$$

and

$$L_i = \log_2 \left(\frac{P(\mathbf{y}, \mathbf{u}^{i-1} | u_i = 0)}{P(\mathbf{y}, \mathbf{u}^{i-1} | u_i = 1)} \right). \quad (6)$$

The bit-channel cutoff rate $R_0(W_N^{(i)})$ is employed as the bias in the stack decoding algorithm.

F. BI-AWGN

For a BI-AWGN channel, the channel cutoff rate is given by [14, p. 142]

$$R_0(W) = 1 - \log_2 \left(1 + e^{\frac{-1}{2\sigma^2}} \right), \quad (7)$$

where σ^2 is the noise variance.

The symmetric capacity $I(W)$ can be approximated as

$$J_{\text{approx}}(t) = \left[1 - 2^{-0.3073 t^{2 \times 0.8935}} \right]^{1.1064}, \quad (8)$$

where $t = \frac{2}{\sigma}$ [15].

Furthermore, the varentropy $V(W)$ can be approximated as [7]

$$V_{\text{approx}}(t) = -(J_{\text{approx}}(t) - 1)^2 - K_{\text{approx}}(t) + 1, \quad (9)$$

where

$$K_{\text{approx}}(t) = \left[1 - 2^{-0.96483 t^{2 \times 0.61746}} \right]^{10.232}. \quad (10)$$

III. POLARIZATION OF CHANNEL PARAMETERS

Following the approach in [9], we assume that the log-likelihood ratio (LLR) of the channel output W follows a Gaussian distribution with mean $2/\sigma^2$ and variance $4/\sigma^2$, and that after each polarization step, the resulting channels continue to behave as BI-AWGN channels. This allows the computation of $\sigma_N^{(i)}$ after $\log_2(N)$ polarization steps for the i th polarized channel. Building on this model, in this paper we use the cutoff rate of the i th bit-channel as

$$R_0(W_N^{(i)}) = 1 - \log_2 \left(1 + e^{\frac{-1}{2(\sigma_N^{(i)})^2}} \right). \quad (11)$$

Similarly, the i th bit-channel mutual information $I(W_N^{(i)})$ can be approximated by $J_{\text{approx}}(t)$, and the bit-channel varentropy can be approximated by $V_{\text{approx}}(t)$, where $t = \frac{2}{\sigma_N^{(i)}}$.

The mean of the i th bit-metric function random variable is [10]

$$\mathbb{E}[\gamma(U_i; \mathbf{Y}, \mathbf{U}^{i-1})] = I(W_N^{(i)}) - R_0(W_N^{(i)}), \quad (12)$$

and its variance is [7]

$$\text{Var}(\gamma(U_i; \mathbf{Y}, \mathbf{U}^{i-1})) = V(W_N^{(i)}). \quad (13)$$

IV. STACK PRUNING METHOD

The defining idea of sequential decoding is that the decoder focuses only on the most promising candidate paths. If a path to a given node appears weak in terms of its metric, we can discard all subsequent paths from that node without causing any meaningful degradation in performance compared to maximum likelihood decoding. The path metric function directs the decoder toward exploring the most promising paths, which naturally brings us to the stack algorithm.

In a PAC code, the convolutional code sees a polarized channel, and most of the synthesized bit channels have very small varentropy, resulting in bit-metric values very close to the polarized channel capacity. In addition to using the path metric function values to order the paths in the stack, we leverage the varentropy polarization by discarding branches

corresponding to an information bit, along with all their descendant paths, if their bit-metric values deviate significantly from their mean.

Using Chebyshev's inequality, the following theorem from [7] demonstrates that the bit-metric random variable of a correct path tends to concentrate around the bit-channel capacity in both nearly noiseless and highly noisy channels.

Theorem 1. [7]. *In a BI-DMC, the bit-metric random variable $\phi(U_i; \mathbf{Y}, \mathbf{U}^{i-1})$ converges to its expected value in probability. More precisely, it holds that*

$$P\left(\left|\gamma(U_i; \mathbf{Y}, \mathbf{U}^{i-1}) - I(W_N^{(i)})\right| \geq m_i\right) \leq \frac{\text{Var}(W_N^{(i)})}{m_i^2}, \quad (14)$$

where m_i is a positive real number.

The following theorem from [7] also proves that the upper bound of (14) converges to zero.

Theorem 2. [7]. *In a BI-DMC, the variances of the bit metric random variables approach zero a.e.*

Moreover, using Chernoff's bound, the following theorem from [10] shows that the probability of the bit-metric random variable deviating significantly from its expected value decays exponentially to zero.

Theorem 3. [10]. *Let $\gamma(U_i; \mathbf{Y}, \mathbf{U}^{i-1})$ represent the bit-metric random variable. For any constant threshold m_T where $m_T < I(W_N^{(i)}) - R_0(W_N^{(i)})$, the probability that $\gamma(U_i; \mathbf{Y}, \mathbf{U}^{i-1})$ falls below m_T is bounded by*

$$P\{\gamma(U_i; \mathbf{Y}, \mathbf{U}^{i-1}) \leq m_T\} \leq 2^{-\frac{m_T}{2}}. \quad (15)$$

Utilizing the upper bounds from (14) and (15), we propose a path-pruning strategy for the stack decoding algorithm as follows. If the bit-metric value $\gamma(u_i; \mathbf{y}, \mathbf{u}^{i-1})$ corresponding to a data bit is less than $\lfloor -(\text{Var}(W_N^{(i)})/P_{th})^{1/2} \rfloor - 10$ or less than $\lfloor \log_2(P_{th}) \rfloor$, then the corresponding branch is not explored and is not inserted into the stack. We define a pruning threshold vector γ_T , whose i th element is given by

$$\gamma_T^{(i)} = \min \left\{ \left\lfloor -\sqrt{\frac{\text{Var}(W_N^{(i)})}{P_{th}}} \right\rfloor - 10, \lfloor \log_2(P_{th}) \rfloor \right\}.$$

V. FAST STACK ALGORITHM

We employ a heap data structure [16], [17], which enables logarithmic-time operations, to implement a memory-efficient stack decoding algorithm for PAC codes. In this structure, partial path metrics serve as the keys, while the satellite data consists of four components: the convolutional code's input vector, output vector, and state; and the polar demapper's intermediate log-likelihood ratios (LLRs). The intermediate LLRs and the convolutional code's input/output vectors are stored in arrays of length $N - 1$ and N , respectively. For an alternative implementation that stores checksum values (instead of the convolutional code's outputs) in a vector of length $N/2$, see [18].

Algorithm 2 presents the main function of our proposed fast stack decoding algorithm for PAC codes. The algorithm

Algorithm 2 PAC-FAST-STACK-DECODER

Input: $\mathbf{L}_{ch}, \mathcal{A}, \mathbf{c}, \mathbf{E}_0, \text{max-cycles}, S\text{-size}, \gamma_T$
Output: $\hat{\mathbf{v}}, \text{cycles}, S\text{-used}$

- 1: $S_values \leftarrow \text{CALCULATE-S-VALUES}(\mathbf{RP})$
- 2: $N \leftarrow \text{length}(\mathbf{L}_{ch})$ ▷ depth of the tree
- 3: $S[1].m \leftarrow 0$
- 4: $S[1].\mathbf{v} \leftarrow \text{NIL}$
- 5: $S[1].\text{st}[1, \dots, |c| - 1] \leftarrow [0, \dots, 0]$
- 6: $S[1].\mathbf{L}[1, \dots, N - 1] \leftarrow [0, \dots, 0]$
- 7: $S[1].\mathbf{u}[1, \dots, N] \leftarrow [0, \dots, 0]$
- 8: $[S_N, \text{cycles}, n] \leftarrow [1, 0, \log_2(N)]$
- 9: **while** True **do**
- 10: **if** $\text{cycles} = \text{max-cycles}$ **then**
- 11: **break**
- 12: **else**
- 13: $\text{cycles} \leftarrow \text{cycles} + 1$
- 14: **end if**
- 15: $[\text{topS}, S, S_N] \leftarrow \text{EXTRACT-MAX}(S, S_N)$
- 16: $\text{st} \leftarrow \text{topS.st}$
- 17: $i \leftarrow \text{length}(\text{topS.v}) + 1$
- 18: $[\mathbf{L}, \text{idx}_{\text{LLR}}, \text{Type}, \text{idx}_{\text{chunk}}, \mathbf{u}] \leftarrow$
 $\text{UPDATELLR}(\mathbf{L}_{ch}, \text{topS.L}, i - 1, \text{topS.u}, n, S_values)$
- 19: $\mathbf{r}_i \leftarrow \mathbf{L}[\text{idx}_{\text{LLR}}]$
- 20: $N_{\text{chunk}} \leftarrow \text{length}(\text{idx}_{\text{chunk}})$
- 21: **if** $\text{Type} = 0$ **then**
- 22: $[S, S_N] \leftarrow \text{F-TYPE-0}(\text{topS}, S, S_N, \text{st}, \mathbf{L}, \text{idx}_{\text{LLR}},$
 $\text{idx}_{\text{chunk}}, \mathbf{u}, \mathbf{c}, \mathbf{E}_0, S\text{-Size}, \mathbf{r}_i, N_{\text{chunk}})$
- 23: **else if** $\text{Type} = \text{REP}$ **then**
- 24: $[S, S_N] \leftarrow \text{F-REP}(\text{topS}, S, S_N, \text{st}, \mathbf{L}, \text{idx}_{\text{LLR}}, \text{idx}_{\text{chunk}},$
 $\mathbf{u}, \mathbf{c}, \mathbf{E}_0, \mathbf{RP}, \gamma_T, S\text{-Size}, \mathbf{r}_i, N_{\text{chunk}})$
- 25: **else if** $\text{Type} = 1$ **then**
- 26: $[S, S_N] \leftarrow \text{F-TYPE-1}(\text{topS}, S, S_N, \text{st}, \mathbf{L}, \text{idx}_{\text{LLR}},$
 $\text{idx}_{\text{chunk}}, \mathbf{u}, \mathbf{c}, \mathbf{E}_0, \gamma_T, S\text{-Size}, \mathbf{r}_i, N_{\text{chunk}})$
- 27: **else if** $\text{Type} = \text{IV}$ **then**
- 28: $[S, S_N] \leftarrow \text{F-TYPE-IV}(\text{topS}, S, S_N, \text{st}, \mathbf{L}, \text{idx}_{\text{LLR}},$
 $\text{idx}_{\text{chunk}}, \mathbf{u}, \mathbf{c}, \mathbf{E}_0, \mathbf{RP}, \gamma_T, S\text{-Size}, \mathbf{r}_i, N_{\text{chunk}})$
- 29: **else if** $\text{Type} = \text{ALL}$ **then**
- 30: $[S, S_N] \leftarrow \text{F-TYPE-ALL}(\text{topS}, S, S_N, \text{st}, \mathbf{L}, \text{idx}_{\text{LLR}},$
 $\text{idx}_{\text{chunk}}, \mathbf{u}, \mathbf{c}, \mathbf{E}_0, \gamma_T, S\text{-Size}, \mathbf{r}_i, N_{\text{chunk}})$
- 31: **end if**
- 32: **if** $\text{length}(S[1].\mathbf{v}) = N$ **then**
- 33: **break**
- 34: **end if**
- 35: **end while**
- 36: $\hat{\mathbf{v}} \leftarrow S[1].\mathbf{v}$
- 37: $S\text{-used} \leftarrow S_N$
- 38: **return** $[\hat{\mathbf{v}}, \text{cycles}, S\text{-used}]$

operates on the channel output LLRs, denoted by \mathbf{L}_{ch} , the data index set \mathcal{A} , the connection polynomial \mathbf{c} , the vector of bit-channel bias values (bit-channel cutoff rates) \mathbf{E}_0 , the maximum number of decoding cycles, the stack size, and the threshold vector γ_T , which determines whether a path should be pruned. The outputs of the algorithm are the data carrier vector $\hat{\mathbf{v}}$, the number of cycles, and the stack size used (i.e., the number of paths stored in the stack).

Based on the rate profile, S_values is defined as a cell array containing $\log_2(N)$ vectors. The first entry consists of a single value representing the total number of information bits K . The second entry is a vector of length two, where the first element denotes the number of information bits K^- in the first half of the codeword and the second element denotes the number of information bits K^+ in the second half. Similarly, the third entry is a vector of length four, with each element

corresponding to the number of information bits in one quarter of the codeword. This subdivision continues hierarchically until the $\log_2(N)$ th entry, where each element corresponds to the number of information bits in a segment of length $N/2^{\log_2(N)} = 1$. The algorithm for computing S_values is presented in Algorithm 8.

The EXTRACT-MAX procedure maintains the heap property and extracts the element $topS$, which corresponds to the path with the largest key (i.e., the highest path-metric value). The variable S_N denotes the number of paths in the stack. The bit index associated with the children of this best path is then stored as i .

In line 18, using Algorithm 7, the UPDATELLR function outputs the updated intermediate LLRs \mathbf{L} ; the index vector for the intermediate LLRs corresponding to the special node, \mathbf{idx}_{LLR} ; the type of the special node, $Type$; the index vector corresponding to the leaf nodes of the special intermediate node, \mathbf{idx}_{chunk} ; and the updated convolutional code's output vector, \mathbf{u} . Then, the intermediate LLRs corresponding to the special node of type $Type$ are stored in the vector \mathbf{r}_i of length N_{chunk} . In lines 21–31, using one of the four types of special nodes, the algorithm updates the stack. The inputs to the special nodes are the stack S ; the stack element corresponding to the best path, $topS$; the number of paths in the stack, S_N ; the state of the convolutional code, \mathbf{st} ; the intermediate LLR vector, \mathbf{L} ; the convolutional code's output vector, \mathbf{u} ; the vector of bias values, \mathbf{E}_0 ; and the indices: (i) the indices of the intermediate LLRs associated with the special node and (ii) the index vector corresponding to the leaf nodes of the special intermediate node. The outputs are the updated stack and the size of the stack. Then the algorithm exits the while loop if decoding has reached level N of the decoding tree.

Algorithm 3 F-TYPE-0 (Rate 0 Node)

Input: $topS, S, S_N, \mathbf{st}, \mathbf{L}, \mathbf{idx}_{LLR}, \mathbf{idx}_{chunk}, \mathbf{u}, \mathbf{c}, \mathbf{E}_0,$
 $S_Size, \mathbf{r}_i, N_{chunk}$
Output: S, S_N

- 1: **for** $n \in \mathbf{idx}_{chunk}$ **do**
- 2: $\mathbf{u}[n] \leftarrow \text{CONVENC}(0, \mathbf{st}, \mathbf{c})$
- 3: $\mathbf{st} \leftarrow [0, \mathbf{st}[1 : c - 1]]$
- 4: **end for**
- 5: $\mathbf{u}_{temp} \leftarrow \text{POLARENCODE}(\mathbf{u}[\mathbf{idx}_{chunk}])$
- 6: $\mathbf{m} \leftarrow 1 - \log_2(1 + \exp(-\mathbf{r}_i \cdot (-1)^{\mathbf{u}_{temp}})) - \mathbf{E}_0[\mathbf{idx}_{chunk}]$
- 7: **if** $S_N = S_Size$ **then**
- 8: $[S, S_N] \leftarrow \text{EXTRACT-MIN}(S, S_N)$
- 9: **end if**
- 10: $S_N \leftarrow S_N + 1$
- 11: $S[S_N].m \leftarrow topS.m + \text{sum}(\mathbf{m})$
- 12: $S[S_N].\mathbf{v} \leftarrow [topS.\mathbf{v}, \mathbf{0}_{1 \times N_{chunk}}]$
- 13: $S[S_N].\mathbf{st} \leftarrow \mathbf{st}$
- 14: $S[S_N].\mathbf{L} \leftarrow \mathbf{L}$
- 15: $S[S_N].\mathbf{u} \leftarrow \mathbf{u}$
- 16: $S \leftarrow \text{HEAPIFY}(S, S_N)$
- 17: **return** $[S, S_N]$

In Algorithm 3, the F-TYPE-0 routine handles a type-0 (rate-0) special node, i.e., a block (chunk) in which all bits are frozen. Lines 1–4 run the one-bit convolutional encoder with input 0 over the indices in \mathbf{idx}_{chunk} , writing the encoder output into $\mathbf{u}[n]$ and advancing the convolutional state \mathbf{st} accordingly. At line 5, the algorithm forms the local partial

sums by $\mathbf{u}_{temp} \leftarrow \text{POLARENCODE}(\mathbf{u}[\mathbf{idx}_{chunk}])$ and computes the bit-metric vector \mathbf{m} , which contains the contributions for the special-node bits. If the stack is full ($S_N = S_Size$), EXTRACT-MIN evicts the worst path. The algorithm then pushes a new path representing the zero decisions over this chunk: it updates the path metric by adding the metric of the partially explored path, appends N_{chunk} zeros to the path vector, stores the updated \mathbf{st} , \mathbf{L} , and \mathbf{u} , and calls HEAPIFY to preserve the heap property.

Algorithm 4 F-REP (Rate $1/N_{chunk}$ Node)

Input: $topS, S, S_N, \mathbf{st}, \mathbf{L}, \mathbf{idx}_{LLR}, \mathbf{idx}_{chunk}, \mathbf{u}, \mathbf{c}, \mathbf{E}_0,$
 $\mathbf{RP}, \gamma_T, S_Size, \mathbf{r}_i, N_{chunk}$
Output: S, S_N

- 1: $\mathbf{RP}_{chunk} \leftarrow \mathbf{RP}[\mathbf{idx}_{chunk}]$
- 2: $p \leftarrow \text{FINDINDICES}(\mathbf{RP}_{chunk}=1)$ ▷ information position
- 3: $\mathbf{V}_0, \mathbf{U}_0, \mathbf{U}_2 \leftarrow \text{zeros}(2, N_{chunk})$
- 4: $\mathbf{V}_0[2][p] \leftarrow 1$ ▷ two candidates: all-zeros and single 1 at position p
- 5: $\mathbf{ST} \leftarrow \text{REPLICATE}(\mathbf{st}, 2)$
- 6: **for** $t = 1$ **to** N_{chunk} **do**
- 7: **for** $j = 1$ **to** 2 **do**
- 8: $\mathbf{U}_0[j][t] \leftarrow \text{CONVENC}(\mathbf{V}_0[j][t], \mathbf{ST}[j], \mathbf{c})$
- 9: **end for**
- 10: $\mathbf{ST} \leftarrow [\mathbf{V}_0[:, t], \mathbf{ST}[:, 1 : c - 1]]$
- 11: **end for**
- 12: $\gamma_{th} \leftarrow \gamma_T[\mathbf{idx}_{chunk}[p]]$
- 13: **for** $j = 1$ **to** 2 **do**
- 14: $\mathbf{U}_2[j][:] \leftarrow \text{POLARENCODE}(\mathbf{U}_0[j][:])$
- 15: $\mathbf{m} \leftarrow 1 - \log_2(1 + \exp(-\mathbf{r}_i \cdot (-1)^{\mathbf{U}_2[j][:]})) - \mathbf{E}_0[\mathbf{idx}_{chunk}]$
- 16: **if** $\mathbf{m}[p] > \gamma_{th}$ **then**
- 17: **if** $S_N = S_Size$ **then**
- 18: $[S, S_N] \leftarrow \text{EXTRACT-MIN}(S, S_N)$
- 19: **end if**
- 20: $S_N \leftarrow S_N + 1$
- 21: $S[S_N].m \leftarrow topS.m + \text{sum}(\mathbf{m})$
- 22: $S[S_N].\mathbf{v} \leftarrow [topS.\mathbf{v}, \mathbf{V}_0[j][:]]$
- 23: $S[S_N].\mathbf{st} \leftarrow \mathbf{ST}[j]$
- 24: $S[S_N].\mathbf{L} \leftarrow \mathbf{L}$
- 25: $\mathbf{u}[\mathbf{idx}_{chunk}] \leftarrow \mathbf{U}_0[j][:]$
- 26: $S[S_N].\mathbf{u} \leftarrow \mathbf{u}$
- 27: $S \leftarrow \text{HEAPIFY}(S, S_N)$
- 28: **end if**
- 29: **end for**
- 30: **return** $[S, S_N]$

In Algorithm 4, the F-REP routine implements the REP special node (rate $1/N_{chunk}$). It also supports an arbitrary placement of the information bit within the portion of the rate profile corresponding to this node. Line 2 stores the position of the information bit in p . The matrices \mathbf{V}_0 , \mathbf{U}_0 , and \mathbf{U}_2 correspond, respectively, to the two candidate inputs to the convolutional encoder, the corresponding convolutional outputs, and the intermediate partial sums at the layer of the REP node. Line 5 replicates the convolutional state vector into \mathbf{ST} to track two candidates: the all-zeros vector and the vector with a single 1 at position p . Lines 6–11 compute, for both candidates, the convolutional outputs across the chunk and update the associated encoder states. Line 12 extracts the bit-metric threshold γ_{th} at the information position from γ_T .

Lines 13–29 then, for each candidate $j \in \{1, 2\}$, form the partial sums via $\text{POLARENCODE}(\mathbf{U}_0[j][:])$, compute the bit-metric vector \mathbf{m} , and compare $\mathbf{m}[p]$ to γ_{th} . If $\mathbf{m}[p] > \gamma_{th}$, the

path is admitted to the stack (evicting the minimum element with EXTRACT-MIN if the stack is full), the path metric is increased, the local decisions $\mathbf{V}_0[j][:]$ are appended, the updated state $\mathbf{ST}[j]$ and buffers are stored, and HEAPIFY restores the heap property. Otherwise, the candidate is discarded. Finally, the algorithm returns the updated stack S and its size S_N .

Algorithm 5 F-TYPE-IV (Rate $2/N_{\text{chunk}}$ Node)

Input: $topS, S, S_N, st, \mathbf{L}, \mathbf{id}_{\text{xLLR}}, \mathbf{id}_{\text{xchunk}}, \mathbf{u}, \mathbf{c}, \mathbf{E}_0,$
 $\mathbf{RP}, \gamma_T, S\text{-Size}, r_i, N_{\text{chunk}}$

Output: S, S_N

- 1: $\mathbf{RP}_{\text{chunk}} \leftarrow \mathbf{RP}[\mathbf{id}_{\text{xchunk}}]$
- 2: $\mathbf{p} \leftarrow \text{FINDINDICES}(\mathbf{RP}_{\text{chunk}}=1)$ \triangleright two information positions
- 3: $\mathbf{V}_0, \mathbf{U}_0, \mathbf{U}_2 \leftarrow \text{zeros}(4, N_{\text{chunk}})$
- 4: $\mathbf{V}_0[1][:] \leftarrow \mathbf{0}$ \triangleright Four candidate input patterns before convolution
- 5: $\mathbf{V}_0[2][p_1] \leftarrow 1$
- 6: $\mathbf{V}_0[3][p_2] \leftarrow 1$
- 7: $\mathbf{V}_0[4][:] \leftarrow \mathbf{RP}_{\text{chunk}}$
- 8: $\mathbf{ST} \leftarrow \text{REPLICATE}(st, 4)$
- 9: **for** $t = 1$ **to** N_{chunk} **do**
- 10: **for** $j = 1$ **to** 4 **do**
- 11: $\mathbf{U}_0[j][t] \leftarrow \text{CONVENC}(\mathbf{V}_0[j][t], \mathbf{ST}[j], \mathbf{c})$
- 12: **end for**
- 13: $\mathbf{ST} \leftarrow [\mathbf{V}_0[:][t], \mathbf{ST}[:, 1:c-1]]$
- 14: **end for**
- 15: $\gamma_{th} \leftarrow \gamma_T[\mathbf{id}_{\text{xchunk}}[p_1]] + \gamma_T[\mathbf{id}_{\text{xchunk}}[p_2]]$
- 16: **for** $j = 1$ **to** 4 **do**
- 17: $\mathbf{U}_2[j][:] \leftarrow \text{POLARENCODE}(\mathbf{U}_0[j][:])$
- 18: $\mathbf{m} \leftarrow 1 - \log_2(1 + \exp(-r_i \cdot (-1)^{\mathbf{U}_2[j][:]}) - \mathbf{E}_0[\mathbf{id}_{\text{xchunk}}])$
- 19: **if** $\mathbf{m}[p_1] + \mathbf{m}[p_2] > \gamma_{th}$ **then**
- 20: **if** $S_N = S\text{-Size}$ **then**
- 21: $[S, S_N] \leftarrow \text{EXTRACT-MIN}(S, S_N)$
- 22: **end if**
- 23: $S_N \leftarrow S_N + 1$
- 24: $S[S_N].m \leftarrow topS.m + \text{sum}(\mathbf{m})$
- 25: $S[S_N].v \leftarrow [topS.v, \mathbf{V}_0[j][:]]$
- 26: $S[S_N].st \leftarrow \mathbf{ST}[j]$
- 27: $S[S_N].L \leftarrow \mathbf{L}$
- 28: $\mathbf{u}[\mathbf{id}_{\text{xchunk}}] \leftarrow \mathbf{U}_0[j][:]$
- 29: $S[S_N].u \leftarrow \mathbf{u}$
- 30: $S \leftarrow \text{HEAPIFY}(S, S_N)$
- 31: **end if**
- 32: **end for**
- 33: **return** $[S, S_N]$

In Algorithm 5, the F-TYPE-IV routine is an extension of F-REP that handles rate $2/N_{\text{chunk}}$ nodes with two information bits. The information-bit positions p_1 and p_2 are obtained from the rate profile restricted to the current chunk. The algorithm evaluates four candidate input patterns: (i) all zeros, (ii) a single 1 at p_1 , (iii) a single 1 at p_2 , and (iv) ones at both $\{p_1, p_2\}$ (i.e., $\mathbf{RP}_{\text{chunk}}$).

Compared with F-REP, the only substantive difference is the admission test: a candidate is kept if the *sum* of the bit-metrics at the two information positions exceeds the *sum* of their thresholds, i.e., $\mathbf{m}[p_1] + \mathbf{m}[p_2] > \gamma_T[p_1] + \gamma_T[p_2]$; otherwise it is pruned. All other steps—convolutional encoding across the chunk, state tracking, forming partial sums via POLARENCODE, heap maintenance through EXTRACT-MIN (when full) and HEAPIFY, and the return values—proceed exactly as in F-REP. At the end, the algorithm returns the updated stack S and its size S_N .

Algorithm 6 F-TYPE-ALL (Rate $N_{\text{chunk}}/N_{\text{chunk}}$ Node)

Input: $topS, S, S_N, st, \mathbf{L}, \mathbf{id}_{\text{xLLR}}, \mathbf{id}_{\text{xchunk}}, \mathbf{u}, \mathbf{c}, \mathbf{E}_0,$
 $\gamma_T, S\text{-Size}, r_i, N_{\text{chunk}}$

Output: S, S_N

- 1: $A_{\text{Size}} \leftarrow 2^{N_{\text{chunk}}}$
- 2: $A, C \leftarrow \text{EMPTYHEAP}()$
- 3: $A[1].m \leftarrow topS.m$
- 4: $A[1].u_d \leftarrow \mathbf{0}_{1 \times N_{\text{chunk}}}$
- 5: $A[1].Len \leftarrow 0$
- 6: $[A_N, count, row_C] \leftarrow [1, 1, 0]$
- 7: **while** $count < A_{\text{Size}}$ **do**
- 8: $[topA, A, A_N] \leftarrow \text{EXTRACT-MAX}(A, A_N)$
- 9: $\mathbf{u}_d \leftarrow topA.u_d$
- 10: $L_{\text{current}} \leftarrow topA.Len + 1$
- 11: $\gamma_{th} \leftarrow \gamma_T[\mathbf{id}_{\text{xchunk}}[L_{\text{current}}]]$
- 12: **for** $b \in \{0, 1\}$ **do**
- 13: $m \leftarrow 1 - \log_2(1 + \exp(-r_i[L_{\text{current}}] \cdot (-1)^b) - \mathbf{E}_0[\mathbf{id}_{\text{xchunk}}[L_{\text{current}}]])$
- 14: **if** $m > \gamma_{th}$ **then**
- 15: $\mathbf{u}_d^{\text{temp}} \leftarrow \mathbf{u}_d$
- 16: $\mathbf{u}_d^{\text{temp}}[L_{\text{current}}] \leftarrow b$
- 17: **if** $L_{\text{current}} < N_{\text{chunk}}$ **then**
- 18: **if** $A_N = S\text{-Size}$ **then**
- 19: $[A, A_N] \leftarrow \text{EXTRACT-MIN}(A, A_N)$
- 20: **end if**
- 21: $A_N \leftarrow A_N + 1$
- 22: $A[A_N].m \leftarrow topA.m + m$
- 23: $A[A_N].u_d \leftarrow \mathbf{u}_d^{\text{temp}}$
- 24: $A[A_N].Len \leftarrow L_{\text{current}}$
- 25: $A \leftarrow \text{HEAPIFY}(A, A_N)$
- 26: **else**
- 27: **if** $row_C = S\text{-Size}$ **then**
- 28: $[C, row_C] \leftarrow \text{EXTRACT-MIN}(C, row_C)$
- 29: **end if**
- 30: $row_C \leftarrow row_C + 1$
- 31: $C[row_C].m \leftarrow topA.m + m$
- 32: $C[row_C].u_d \leftarrow \mathbf{u}_d^{\text{temp}}$
- 33: $C \leftarrow \text{HEAPIFY}(C, row_C)$
- 34: $count \leftarrow count + 1$
- 35: **end if**
- 36: **else**
- 37: $count \leftarrow count + 2^{(N_{\text{chunk}} - L_{\text{current}})}$
- 38: **end if**
- 39: **end for**
- 40: **end while**
- 41: **for** $k = 1$ **to** row_C **do**
- 42: $[topC, C, row_C] \leftarrow \text{EXTRACT-MAX}(C, row_C)$
- 43: $\mathbf{U}_0 \leftarrow \text{POLARENCODE}(topC.u_d)$
- 44: $\mathbf{V}_0 \leftarrow \mathbf{0}_{1 \times N_{\text{chunk}}}$
- 45: $st^{\text{temp}} \leftarrow st$
- 46: **for** $t = 1$ **to** N_{chunk} **do**
- 47: $\mathbf{V}_0[t] \leftarrow \text{CONVENCINV}(\mathbf{U}_0[t], st^{\text{temp}}, \mathbf{c})$
- 48: $st^{\text{temp}} \leftarrow [\mathbf{V}_0[t], st^{\text{temp}}[1:c-1]]$
- 49: **end for**
- 50: **if** $S_N = S\text{-Size}$ **then**
- 51: $[S, S_N] \leftarrow \text{EXTRACT-MIN}(S, S_N)$
- 52: **end if**
- 53: $S_N \leftarrow S_N + 1$
- 54: $S[S_N].m \leftarrow topC.m$
- 55: $S[S_N].v \leftarrow [topS.v, \mathbf{V}_0]$
- 56: $S[S_N].st \leftarrow st^{\text{temp}}$
- 57: $S[S_N].L \leftarrow \mathbf{L}$
- 58: $\mathbf{u}^{\text{temp}} \leftarrow \mathbf{u}$
- 59: $\mathbf{u}^{\text{temp}}[\mathbf{id}_{\text{xchunk}}] \leftarrow \mathbf{U}_0$
- 60: $S[S_N].u \leftarrow \mathbf{u}^{\text{temp}}$
- 61: $S \leftarrow \text{HEAPIFY}(S, S_N)$
- 62: **end for**
- 63: **return** $[S, S_N]$

In Algorithm 6, the F-TYPE-ALL routine implements the rate-1 (all-information) special node. The maximum number of paths in the chunk subtree is $A_{\text{Size}} \triangleq 2^{N_{\text{chunk}}}$. We maintain two heaps: A for frontier (partial) paths and C for completed length- N_{chunk} paths.

Lines 7–40 implement a heap exploration of the subtree in which every bit is an information bit. At each expansion step, for the current position L_{current} and branch $b \in \{0, 1\}$, the bit-metric m is computed and compared against the corresponding threshold γ_{th} . If $m > \gamma_{th}$, the child is admitted: if $L_{\text{current}} < N_{\text{chunk}}$, it is pushed into A with updated metric and length; otherwise, the fully specified path is pushed into C . If $m \leq \gamma_{th}$, the branch is pruned and its remaining subtree is skipped by increasing $count$ by $2^{(N_{\text{chunk}} - L_{\text{current}})}$. In this algorithm, we assume a maximum stack size of S_{Size} for both A and C . When either heap is full, EXTRACT-MIN is used to evict the worst path before admitting a new one.

Lines 41–62 process completed candidates from C in descending metric order. For each, \mathbf{U}_0 is formed via POLARENCODE(\cdot); the corresponding convolutional input \mathbf{V}_0 and updated state $\mathbf{st}^{\text{temp}}$ are recovered across the chunk using CONVENCINV, an inverse operation of the 1-bit convolutional code. The resulting full-path is then appended to the global stack S (with EXTRACT-MIN if needed) and HEAPIFY restores the heap property. Finally, the algorithm returns the updated stack S and its size S_N .

Algorithm 7 updates the intermediate LLRs. The inputs are the channel LLRs \mathbf{L}_{ch} , the intermediate LLRs \mathbf{L} , the running path bit index i , the convolutional code output vector \mathbf{u} , the tree depth $n = \log_2 N$, and the precomputed S_values (Alg. 8). The outputs are the updated \mathbf{L} ; $\mathbf{idx}_{\text{LLR}}$, the index vector for the intermediate LLRs corresponding to the special node; the type of the special node; $\mathbf{idx}_{\text{chunk}}$, the index vector corresponding to the leaf nodes of the special intermediate node; and the updated vector \mathbf{u} . The LLRs can be updated as [1]

$$f(\mathbf{L}^{(L)}, \mathbf{L}^{(R)}) = 2 \tanh^{-1} \left(\tanh\left(\frac{\mathbf{L}^{(L)}}{2}\right) \tanh\left(\frac{\mathbf{L}^{(R)}}{2}\right) \right), \quad (16)$$

$$g(\mathbf{L}^{(L)}, \mathbf{L}^{(R)}, \mathbf{u}_n) = \mathbf{L}^{(L)} (-1)^{\mathbf{u}_n} + \mathbf{L}^{(R)}.$$

The variable $s \in \{0, 1, \dots, n-1\}$ denotes the depth in the polarization tree (with $s = 0$ at the leaves). The variable sel determines whether the f or g function is used: $sel = 0$ uses g , and $sel = 1$ uses f . If $i = 0$, the algorithm starts from the root ($s \leftarrow n-1$) and uses the f function first ($sel \leftarrow 1$). Otherwise, the depth is determined by find-first-bit-set (ffs) operation introduced in [19]. To apply the g function, we compute the checksum \mathbf{u}_n at depth s by polar-encoding the segment $\mathbf{u}[i-2^s+1:i]$ (lines 14 and 29). The algorithm then applies f or g to the parent-node LLRs: in lines 12–24 the parent LLRs come from the channel, and in lines 26–38 from the intermediate LLRs \mathbf{L} . The selector is flipped to f ($sel \leftarrow 1$) for the next lower stage.

After updating the LLRs at a depth of the polarization tree, the algorithm locates the *chunk* that contains index i and obtains, from the precomputed partition summary S_values , the number of information bits in this chunk (line 42). If $Type \in \{0, 1, 2, \text{chunk_size}\}$, the algorithm identifies a special

Algorithm 7 UPDATELLR

Input: $\mathbf{L}_{ch}, \mathbf{L}, i, \mathbf{u}, n, S_values$
Output: $\mathbf{L}, \mathbf{idx}_{\text{LLR}}, Type, \mathbf{idx}_{\text{chunk}}, \mathbf{u}$

```

1:  $\mathbf{idx}_{\text{LLR}} \leftarrow []$ 
2:  $N \leftarrow 2^n$ 
3: if  $i = 0$  then
4:    $s \leftarrow n - 1$ 
5:    $sel \leftarrow 1$  ▷  $f$  function
6: else
7:    $s \leftarrow \text{ffs}(i)$  ▷ depth:  $0, 1, \dots, n-1$  ( $0$  is leaf)
8:    $sel \leftarrow 0$  ▷  $g$  function
9: end if
10: while  $s \geq 0$  do
11:    $\text{two}_s \leftarrow 2^s$ 
12:   if  $s = n - 1$  then
13:     if  $i > 0 \wedge sel = 0$  then
14:        $\mathbf{u}_n \leftarrow \text{POLARENCODE}(\mathbf{u}[i - \text{two}_s + 1 : i])$ 
15:     end if
16:      $\mathbf{L}^{(L)} \leftarrow \mathbf{L}_{ch}[1 : \text{two}_s]$ ,
17:      $\mathbf{L}^{(R)} \leftarrow \mathbf{L}_{ch}[\text{two}_s + 1 : 2\text{two}_s]$ 
18:     if  $sel = 1$  then
19:        $\mathbf{L}[1 : \text{two}_s] \leftarrow f(\mathbf{L}^{(L)}, \mathbf{L}^{(R)})$ 
20:     else
21:        $\mathbf{L}[1 : \text{two}_s] \leftarrow g(\mathbf{L}^{(L)}, \mathbf{L}^{(R)}, \mathbf{u}_n)$ 
22:     end if
23:      $\mathbf{idx}_{\text{LLR}} \leftarrow [1 : \text{two}_s]$ 
24:      $sel \leftarrow 1$ 
25:   else
26:      $\text{shift\_out} \leftarrow N - 2^{s+1}$ ,
27:      $\text{shift\_in} \leftarrow N - 2^{s+2}$ 
28:     if  $i > 0 \wedge sel = 0$  then
29:        $\mathbf{u}_n \leftarrow \text{POLARENCODE}(\mathbf{u}[i - \text{two}_s + 1 : i])$ 
30:     end if
31:      $\text{shift}_L \leftarrow \text{shift\_in} + [1 : \text{two}_s]$ 
32:      $\text{shift}_R \leftarrow \text{shift\_in} + \text{two}_s + [1 : \text{two}_s]$ 
33:      $\mathbf{idx}_{\text{LLR}} \leftarrow \text{shift\_out} + [1 : \text{two}_s]$ 
34:     if  $sel = 1$  then
35:        $\mathbf{L}[\mathbf{idx}_{\text{LLR}}] \leftarrow f(\mathbf{L}[\text{shift}_L], \mathbf{L}[\text{shift}_R])$ 
36:     else
37:        $\mathbf{L}[\mathbf{idx}_{\text{LLR}}] \leftarrow g(\mathbf{L}[\text{shift}_L], \mathbf{L}[\text{shift}_R], \mathbf{u}_n)$ 
38:     end if
39:      $sel \leftarrow 1$ 
40:      $\text{idx} \leftarrow \left\lfloor \frac{i+1}{\text{two}_s} \right\rfloor$ 
41:      $\text{level} \leftarrow n - s + 1$ 
42:      $Type \leftarrow S\_values\{\text{level}\}(\text{idx})$ 
43:      $\text{chunk\_size} \leftarrow \frac{N}{2^{\text{level}-1}}$ 
44:     if  $Type \in \{0, 1, 2, \text{chunk\_size}\}$  then
45:        $\text{start} \leftarrow (\text{idx} - 1) \cdot \text{chunk\_size} + 1$ 
46:        $\text{end} \leftarrow \text{idx} \cdot \text{chunk\_size}$ 
47:        $\mathbf{idx}_{\text{chunk}} \leftarrow [\text{start} : \text{end}]$ 
48:       break
49:     end if
50:   end if
51:    $s \leftarrow s - 1$ 
52: end while
53: return  $[\mathbf{L}, \mathbf{idx}_{\text{LLR}}, Type, \mathbf{idx}_{\text{chunk}}, \mathbf{u}]$ 

```

node and exits the loop early. This enables the caller (the fast stack decoder) to switch to a node-specialized routine for the detected chunk. At each visited stage, the algorithm records the updated LLR block in $\text{id}\mathbf{x}_{\text{LLR}}$, ensuring the caller knows exactly which entries of \mathbf{L} changed. It finally returns $(\mathbf{L}, \text{id}\mathbf{x}_{\text{LLR}}, \text{Type}, \text{id}\mathbf{x}_{\text{chunk}}, \mathbf{u})$.

Algorithm 8 CALCULATE-S-VALUES

Input: \mathbf{RP}
Output: S_values

- 1: $N \leftarrow \text{length}(\mathbf{RP})$
- 2: $\text{max_depth} \leftarrow \log_2(N)$
- 3: $S_values \leftarrow \text{cell}(\text{max_depth} + 1, 1)$
- 4: $S_values\{1\} \leftarrow \text{sum}(\mathbf{RP})$ ▷ root node at depth 0
- 5: **for** $d = 1 \rightarrow \text{max_depth}$ **do**
- 6: $\text{num_nodes} \leftarrow 2^d$
- 7: $S_values\{d+1\} \leftarrow \mathbf{0}_{1 \times \text{num_nodes}}$
- 8: **for** $i = 0 \rightarrow \text{num_nodes} - 1$ **do**
- 9: $\text{start} \leftarrow i \cdot \frac{\text{num_nodes}}{N} + 1$
- 10: $\text{end} \leftarrow (i + 1) \cdot \frac{\text{num_nodes}}{N}$
- 11: $S_values\{d+1\}[i+1] \leftarrow \text{sum}(\mathbf{RP}[\text{start} : \text{end}])$
- 12: **end for**
- 13: **end for**
- 14: **return** S_values

In Algorithm 8, the procedure computes the hierarchical distribution of information bits across different segments of the codeword based on the given rate profile \mathbf{RP} . The algorithm constructs S_values as a cell array with $\log_2(N) + 1$ entries, where N is the codeword length. The first entry, $S_values\{1\}$, stores the total number of information bits K , obtained by summing all elements of \mathbf{RP} . For each subsequent depth level $d = 1, 2, \dots, \log_2(N)$, the algorithm divides the codeword into 2^d equally sized segments and computes the number of information bits within each segment. Thus, $S_values\{d+1\}$ is a vector of length 2^d , where the i -th element corresponds to the number of information bits in the i -th segment of length $N/2^d$. This hierarchical representation captures the distribution of information bits from the entire codeword down to individual bit positions.

VI. NUMERICAL RESULTS

In this section, we evaluate the performance of our proposed decoding schemes over a BI-AWGN channel with BPSK modulation. Since a Fano decoder with frame error rate (FER) D at a given E_b/N_0 achieves performance very close to the theoretical bounds for the short block lengths considered, we set the threshold parameter to $P_{\text{th}} = D/10$ in our numerical results. For all evaluations, we adopt the connection polynomial $c(t) = t^{10} + t^9 + t^7 + t^3 + 1$ [3]. Furthermore, for Fano decoding, we fix the threshold spacing to $\Delta = 2$.

Fig. 1 compares the performance of the conventional stack decoding algorithm for a PAC(128,64) code with the performance of the path-pruning strategy in stack decoding (PstackD) proposed by [10] and our proposed path-pruning strategy, which leverages bit-channel variances (PstackD-Var). The average number of paths in the stack is also compared in this figure. At an E_b/N_0 value of 1 dB, our proposed pruning method achieves a 70% reduction in the average number of

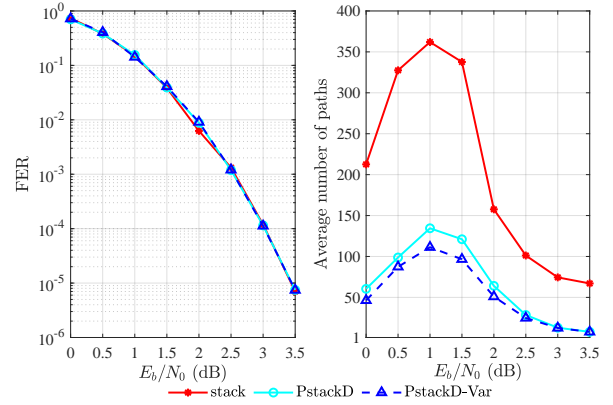


Fig. 1. FER performance and the average number of paths in the stack comparison of PAC(128,64) codes with different path-pruning strategies for the stack decoding algorithm.

paths in the stack compared to the conventional stack decoding algorithm, and an 18% reduction compared to the method in [10].

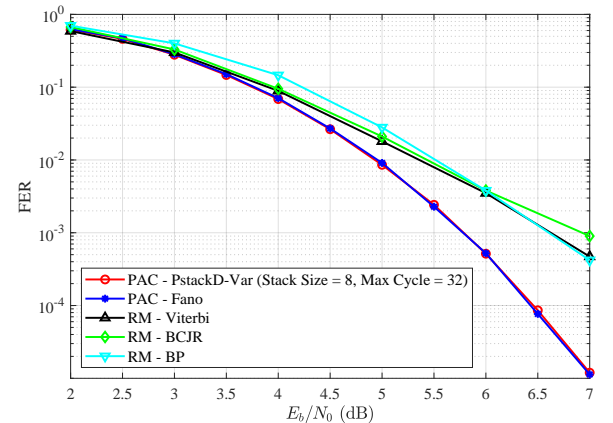


Fig. 2. FER performance comparison of PAC(64,57) and RM(64,57) codes under different decoding algorithms.

Fig. 2 illustrates the FER performance of the PAC(64,57) code decoded using our proposed fast stack decoding algorithm with a stack size of 8 and a maximum of 32 decoding cycles, compared against Fano decoding, where no limit is imposed on the number of explored paths. For comparison, we also evaluate the FER performance of the corresponding RM(64,57) code under Viterbi, BCJR, and BP decoding as in [20]. It can be observed that while Viterbi and BCJR decoding provide near-ML performance, their computational complexity grows exponentially with the number of frozen bits, making them impractical for larger block lengths.

Table I also reports the average number of decoding cycles, the average stack size used, and the average number of times the f and g functions are invoked. For reference, in conventional SC decoding of polar codes, the f and g functions are called exactly $2N - 2 = 126$ times for a code length

TABLE I
AVERAGE PERFORMANCE METRICS OF PSTACKD-VAR DECODER FOR PAC(64, 57) (STACK SIZE = 8, MAX CYCLES = 32)

E_b/N_0 (dB)	2.0	2.5	3.0	3.5	4.0	4.5	5.0	5.5	6.0	6.5	7.0
Average Cycles	16.04	16.59	16.71	16.29	15.72	15.35	15.14	15.04	15.01	15.00	15.00
Average Stack Used	6.68	6.50	6.03	5.41	4.76	4.12	3.84	3.54	3.21	2.90	2.76
Average f & g Operations	30.25	31.35	31.55	30.66	29.48	28.72	28.28	28.09	28.02	28.00	28.00

TABLE II
AVERAGE PERFORMANCE METRICS OF PSTACKD-VAR DECODER FOR PAC(128, 99) (STACK SIZE = 64, MAX CYCLES = 1024)

E_b/N_0 (dB)	0.0	0.5	1.0	1.5	2.0	2.5	3.0	3.5	4.0	4.5	5.0
Average Cycles	37.87	42.02	53.47	81.01	110.96	95.38	65.29	44.88	37.47	35.47	35.08
Average Stack Used	24.63	22.86	23.98	29.02	31.79	26.05	19.44	14.29	11.63	10.65	9.69
Average f & g Operations	74.11	82.66	106.05	161.76	222.32	191.15	130.12	88.30	73.08	68.96	68.16

of $N = 64$. In contrast, for stack decoding, multiple candidate paths are maintained simultaneously, and the reported averages in the table are computed per decoded codeword, representing the total number of f and g function calls accumulated across all explored paths during the decoding process.

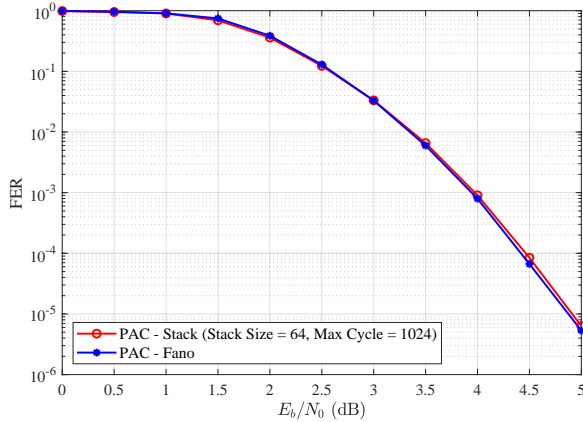


Fig. 3. FER performance comparison of PAC(128, 99) codes with Fano and stack decoding algorithms.

Fig. 3 illustrates the FER performance of the proposed stack decoding algorithm with a stack size of 64 and a maximum of 1024 decoding cycles. The results demonstrate that the proposed approach achieves FER performance comparable to that of the Fano sequential decoding algorithm.

Table II also presents the average number of decoding cycles, the average stack size used, and the average number of times the f and g functions are invoked for the PAC(128, 99) code. For reference, in conventional SC decoding of polar codes, the f and g functions are called exactly $2N - 2 = 254$ times for a code length of $N = 128$.

VII. CONCLUSION

In this paper, we introduced a fast stack decoding algorithm for PAC codes that efficiently handles rate-0, REP, type-IV, and rate-1 special nodes. For a rate-1 node with N_0 leaf nodes in the polarization tree, a conventional stack decoder may need to explore up to 2^{N_0} candidate paths, which becomes prohibitively complex for high-rate codes. In contrast, unlike the

fast list decoding algorithm that restricts exploration to only $2L$ paths for a list size of L , the proposed approach addresses the computational challenge of rate-1 nodes for the fast stack decoding more effectively. To tackle this issue, we leverage the polarization properties of the bit-metric function and introduce a novel pruning criterion that selectively discards low-probability paths while ensuring that the probability of pruning the correct path decreases exponentially. Furthermore, we propose an accurate approximation method for estimating the polarized varentropy over BI-AWGN channels, enabling the design of adaptive and efficient pruning thresholds.

REFERENCES

- [1] E. Arkan, "Channel polarization: A method for constructing capacity-achieving codes for symmetric binary-input memoryless channels," *IEEE Transactions on information Theory*, vol. 55, no. 7, pp. 3051–3073, 2009.
- [2] —, "From sequential decoding to channel polarization and back again," *arXiv preprint arXiv:1908.09594*, 2019.
- [3] M. Moradi, A. Mozammel, K. Qin, and E. Arkan, "Performance and complexity of sequential decoding of PAC codes," *arXiv preprint arXiv:2012.04990*, 2020.
- [4] M. Moradi, "Polarization-adjusted convolutional (PAC) codes as a concatenation of inner cyclic and outer polar-and Reed-Muller-like codes," *Finite Fields and Their Applications*, vol. 93, p. 102321, 2024.
- [5] K. Zigangirov, "Some sequential decoding procedures," *Problemy Peredachi Informatsii*, vol. 2, no. 4, pp. 13–25, 1966.
- [6] F. Jelinek, "Fast sequential decoding algorithm using a stack," *IBM journal of research and development*, vol. 13, no. 6, pp. 675–685, 1969.
- [7] M. Moradi and H. Mahdaviyar, "On fast SC-based polar decoders: Metric polarization and a pruning technique," *arXiv preprint arXiv:2408.03840*, 2024.
- [8] I. Tal and A. Vardy, "How to construct polar codes," *IEEE Transactions on Information Theory*, vol. 59, no. 10, pp. 6562–6582, 2013.
- [9] H. Li and J. Yuan, "A practical construction method for polar codes in AWGN channels," in *IEEE 2013 Tencon - Spring*, 2013, pp. 223–226.
- [10] M. Moradi and A. Mozammel, "A tree pruning technique for decoding complexity reduction of polar codes and PAC codes," *IEEE Transactions on Communications*, vol. 71, no. 5, pp. 2576–2586, 2023.
- [11] G. Trofimuk, N. Iakuba, S. Rets, K. Ivanov, and P. Trifonov, "Fast block sequential decoding of polar codes," *IEEE Transactions on Vehicular Technology*, vol. 69, no. 10, pp. 10988–10999, 2020.
- [12] X. Yao and X. Ma, "Low-complexity PSCL decoding of polar codes," *IEEE Transactions on Communications*, pp. 1–1, 2025.
- [13] M. Moradi, "On sequential decoding metric function of polarization-adjusted convolutional (PAC) codes," *IEEE Transactions on Communications*, vol. 69, no. 12, pp. 7913–7922, 2021.
- [14] A. J. Viterbi and J. K. Omura, *Principles of digital communication and coding*. Courier Corporation, 2009.
- [15] F. Brannstrom, *Convergence analysis and design of multiple concatenated codes*. Ph.D. dissertation, Chalmers University, 2004.
- [16] T. H. Cormen, C. E. Leiserson, R. L. Rivest, and C. Stein, *Introduction to algorithms*. MIT press, 2009.

- [17] O. Shalvi, N. Sommer, and M. Feder, "Signal codes: Convolutional lattice codes," *IEEE Transactions on Information Theory*, vol. 57, no. 8, pp. 5203–5226, 2011.
- [18] M. Moradi, "Performance and computational analysis of polarization-adjusted convolutional (PAC) codes," Ph.D. dissertation, Bilkent Universitesi (Turkey), 2022.
- [19] C. Leroux, A. J. Raymond, G. Sarkis, I. Tal, A. Vardy, and W. J. Gross, "Hardware implementation of successive-cancellation decoders for polar codes," *Journal of Signal Processing Systems*, vol. 69, no. 3, pp. 305–315, 2012.
- [20] E. Arıkan, H. Kim, G. Markarian, U. Ozgur, and E. Poyraz, "Performance of short polar codes under ML decoding," *Proc. ICT MobileSummit, (Santander, Spain)*, pp. 10–12, 2009.